

Published in final edited form as:

*Biochemistry*. 2012 April 17; 51(15): 3232–3240. doi:10.1021/bi3001984.

## A constitutively active $G\alpha$ subunit provide insights into the mechanism of G protein activation

Garima Singh<sup>†</sup>, Sekar Ramachandran<sup>†</sup>, and Richard A. Cerione<sup>\*</sup>

Departments of Molecular Medicine and Chemistry and Chemical Biology, Cornell University, Ithaca, New York 14853

### Abstract

The activation of  $G\alpha$  subunits of heterotrimeric G proteins by G protein-coupled receptors (GPCRs) is a critical event underlying a variety of biological responses. Understanding how G proteins are activated will require structural and biochemical analyses of GPCRs complexed to their G protein partners, together with structure-function studies of  $G\alpha$  mutants that shed light on the different steps in the activation pathway. Previously, we reported that the substitution of a glycine for a proline at position 56 within the linker region connecting the helical and GTP-binding domains of a  $G\alpha$  chimera, designated  $\alpha T^*$ , yields a more readily exchangeable state for guanine nucleotides. Here we show that GDP-GTP exchange on  $\alpha T^*(G56P)$ , in the presence of the light-activated GPCR, rhodopsin ( $R^*$ ), is less sensitive to the  $\beta 1\gamma 1$  subunit complex as compared to wild-type  $\alpha T^*$ . We solved the x-ray crystal structure for the  $\alpha T^*(G56P)$  mutant and found that the G56P substitution leads to concerted changes that are transmitted to the conformationally sensitive switch regions, the  $\alpha 4/\beta 6$  loop, and the  $\beta 6$  strand. The  $\alpha 4/\beta 6$  loop has been proposed to be a GPCR contact site that signals to the TCAT motif and weakens the binding of the guanine ring of GDP, whereas, the switch regions are the contact sites for the  $\beta 1\gamma 1$  complex. Collectively, these biochemical and structural data lead us to suggest that  $\alpha T^*(G56P)$  may be adopting a conformation that is normally induced within  $G\alpha$  subunits by the combined actions of a GPCR and a  $G\beta\gamma$  subunit complex during the G protein activation event.

Transducin is a heterotrimeric guanine nucleotide-binding protein (G protein) that is located in the outer segments of retinal rod cells (reviewed in refs. 1 and 2). In the visual phototransduction cascade, light-activated rhodopsin ( $R^*$ ) catalyzes GDP-GTP exchange on the  $G\alpha$  subunit of transducin ( $\alpha T$ ). The activated GTP-bound  $\alpha T$  subunit converts the signal (i.e. a photon of light) into the final sensory output (the hyperpolarization of rod outer segment membranes and the visual response) by coupling the light-dependent activation of rhodopsin to the stimulation of the effector enzyme, the cGMP phosphodiesterase (PDE). This reduces the concentrations of cGMP in retinal rod cells and results in the closure of cGMP-gated ion channels and membrane hyperpolarization. The GTP hydrolytic activity of  $\alpha T$  returns it to the basal GDP-bound state allowing the rebinding of the  $G\beta\gamma$  subunit complex (i.e.  $\beta 1\gamma 1$ ). The rate of GTP hydrolysis can be modulated by the PDE and markedly increased by RGS (Regulators of G protein-signaling) proteins.<sup>3</sup>

The  $\alpha T$  subunit, like other  $G\alpha$  subunits of the heterotrimeric G protein superfamily, has a conserved nucleotide-binding (GTPase) domain similar to that of Ras and other “small G proteins”, and a helical domain connected by flexible linkers that bury the bound guanine nucleotide.<sup>4,5</sup> High-resolution structural information has been obtained from x-ray

<sup>\*</sup>To whom correspondence should be addressed: Department of Molecular Medicine, College of Veterinary Medicine, Cornell University, Ithaca, NY 14853-6401. Tel: (607) 253-3888. Fax: (607) 253-3659, rac1@cornell.edu.

<sup>†</sup>These authors have contributed equally to this work.

crystallographic structures of various G $\alpha$  subunits alone,<sup>4-9</sup> in complex with their G $\beta\gamma$  partners,<sup>10,11</sup> as well as with their effector proteins.<sup>12,13</sup> These structures have highlighted the presence of three flexible regions, referred to as switch regions, in the GTPase domain that undergo conformational changes in response to the binding of GTP.

The x-ray crystal structure of the Gs heterotrimer complexed to the  $\beta$ 2-adrenergic receptor has been recently achieved.<sup>14-16</sup> In this structure, the C-terminal end of the  $\alpha$ 5-helix of the G $\alpha$  subunit (referred to as G $\alpha$ s) makes extensive contacts with the GPCR, confirming biochemical studies using synthetic peptides and mutants of G $\alpha$  subunits that suggested the binding site for GPCRs on their G $\alpha$  subunits is located at the C-terminal  $\alpha$ -helix of G $\alpha$ .<sup>17-20</sup> The x-ray structure for the  $\beta$ 2-adrenergic receptor-Gs complex also confirmed predictions from molecular modeling studies that the binding site on the G $\alpha$  subunit for the GPCR is separated from the guanine nucleotide-binding (GTPase) domain by  $\sim$ 30 Å.<sup>21</sup>

Given this distance, a question of great interest has been how GPCRs are able to transmit changes to the guanine nucleotide-binding sites of their G $\alpha$ -signaling partners that weaken the binding of GDP and thereby stimulate the rate-limiting step for G protein activation, namely GDP-GTP exchange. In this regard, the x-ray crystal structure of the  $\beta$ 2-adrenergic receptor complexed to the heterotrimeric G protein Gs provides an atomic resolution model of the endpoint of G protein activation, subsequent to nucleotide release, and suggests that a significant displacement of the helical-domain from the GTPase domain may be an important contributor to GDP-GTP exchange.<sup>14</sup> However, the development of constitutively active G $\alpha$  mutants that are able to exchange GDP for GTP at a relatively rapid rate in the absence of a GPCR,<sup>22-25</sup> together with EPR studies of R\* $\alpha$ T interactions,<sup>26,27</sup> have also added to the picture by defining the distinct steps that underlie GPCR-dependent G protein activation. The results obtained thus far point to the involvement of the  $\alpha$ 5 helix and the  $\beta$ 6/ $\alpha$ 5 loop within G $\alpha$  subunits in helping GPCRs to stimulate GDP dissociation. In particular, movements in the  $\beta$ 6 loop and the  $\beta$ 2- $\beta$ 3 turn of G $\alpha$  subunits have been suggested to be important for GPCR-stimulated GDP-GTP exchange by EPR studies where mutations that caused the  $\beta$ 2- $\beta$ 3 strands to move away from the  $\alpha$ 5 helix led to increases in the basal guanine nucleotide exchange activity of the G $\alpha$ i1 subunit, whereas mutations within the  $\beta$ 6 strand resulted in a decrease in the nucleotide exchange rates.<sup>26</sup> Mutational and computational studies have further suggested that a GPCR-induced movement of the  $\alpha$ 5 helix of G $\alpha$  subunits can be relayed to the GDP-binding site through the N-terminal  $\alpha$  helix and the  $\beta$ 2- $\beta$ 3 strands.<sup>23,28,29</sup> Moreover, recent EPR studies suggest that engagement of the  $\beta$ 6/ $\alpha$ 5 loop by GPCRs can be translated into significant changes in the juxtaposition of the helical domain relative to the guanine nucleotide-binding (GTPase) domain which help to provide an “escape route” for GDP.<sup>27</sup>

Still, there are a number of additional questions surrounding the steps that make-up the complete reaction pathway for a G protein activation event that will likely require the combined efforts of solution and crystallographic analyses, as well as biochemical studies of GPCR-G protein complexes and different G $\alpha$  mutants that will mirror different steps of the pathway. For example, what role does the G $\beta\gamma$  subunit complex play in different stages of G protein activation? It was known for several years that G $\beta\gamma$  increased the affinity of GPCRs for their G $\alpha$  subunit targets and this was traditionally felt to be the primary role for G $\beta\gamma$  in GPCR-stimulated nucleotide exchange. However, there have been suggestions that the G $\beta\gamma$  subunit complex has a direct involvement in the G protein activation event.<sup>30-33</sup> Indeed, mutagenesis studies have pointed to a potentially more direct role for G $\beta\gamma$  in stimulating nucleotide exchange, leading to a model where the G $\beta\gamma$  complex works together with GPCRs to catalyze GDP-GTP exchange by helping to create an “exit” for GDP release by influencing the interactions between the helical and GTPase domains of the G $\alpha$  subunit.<sup>34</sup>

Previous work from our laboratory showed that point mutations made within the linker regions that connect the helical and GTPase domains of a chimeric  $G\alpha$  subunit, comprised primarily of the  $\alpha T$  subunit and a short segment of  $G\alpha i1$  (designated as  $\alpha T^*$ ), resulted in an accelerated exchange of GDP for GTP.<sup>25</sup> In order to better understand how one such mutant,  $\alpha T^*(G56P)$ , was capable of undergoing constitutive GDP-GTP exchange (i.e. independent of light-activated rhodopsin), and what this might tell us about the G protein activation event, we set out to further characterize its nucleotide exchange activity under various conditions, as well as solve its x-ray crystal structure. Here we show that the  $\alpha T^*(G56P)$  mutant can be strongly activated in the absence of  $G\beta\gamma$  ( $\beta 1\gamma 1$ ) when assayed together with sufficiently high levels of rhodopsin, thus differing from the case of wild-type  $\alpha T^*$  (designated  $\alpha T^*(WT)$ ) which exhibits a much greater dependence on  $\beta 1\gamma 1$  for full activation. This suggested that the  $\alpha T^*(G56P)$  mutant might exist in a conformational state that bears some similarity to that normally induced within the  $\alpha T^*(WT)$  subunit by  $G\beta\gamma$  during the activation event. We were able to solve a 2.9 Å resolution x-ray crystal structure for GDP-bound  $\alpha T^*(G56P)$  and found that it showed more similarity (particularly in Switch 1) to the activated, GTP $\gamma$ S-bound state of  $\alpha T^*(WT)$  rather than to the GDP-bound form of  $\alpha T^*(WT)$ . Overall, these findings raise some intriguing possibilities regarding how  $G\beta\gamma$  might work together with a GPCR during the G protein activation event, as well as corroborate some earlier suggestions from NMR studies that  $G\beta\gamma$  complexes may help to impart “activating conformational changes” within  $G\alpha$  subunits.<sup>30</sup>

## Experimental Procedures

### Protein expression and purification

The linker mutation (G56P) described in this study was made in the  $\alpha T^*$  background as previously reported.<sup>25</sup> The recombinant  $\alpha T^*(WT)$  and  $\alpha T^*(G56P)$  mutant were expressed in BL21 (DE3) supercompetent cells and purified in the presence of 50  $\mu$ M GDP as described previously.<sup>35</sup> The recombinant proteins were further purified by gel filtration chromatography on a HiLoad Superdex 75 HR26/60 column equilibrated with a buffer containing 20 mM Na-HEPES, pH 7.5, and 10% glycerol. The samples were aliquoted, snap-frozen, and stored at  $-80^\circ\text{C}$ . The final yield of recombinant  $\alpha T^*$  proteins ranged from 3 to 5 mg of pure protein/liter of bacterial culture. Retinal  $\alpha T$  and the  $\beta 1\gamma 1$  complex were purified from bovine retina as described.<sup>25</sup> Urea-washed rod outer segment membranes were prepared as described.<sup>36</sup>

### [<sup>35</sup>S]GTP $\gamma$ S-binding assays

Rhodopsin, together with the  $\alpha T^*$  subunits and  $\beta 1\gamma 1$ , was incubated in HMDN buffer (20 mM HEPES, pH 7.5, 5 mM  $\text{MgCl}_2$ , 1 mM dithiothreitol, and 100 mM NaCl) for 20 minutes at room temperature and in room light. [<sup>35</sup>S]GTP $\gamma$ S (final concentration, 5  $\mu$ M; specific activity, 1 Ci/mmol) was added to initiate the reaction, and the samples were incubated for different time periods. The reaction was quenched by direct application to pre-wetted nitrocellulose filters (Schleicher & Schuell; pore size, 0.45  $\mu$ m) on a suction manifold. The filters were washed twice with HMN buffer (20 mM HEPES, pH 7.5, 5 mM  $\text{MgCl}_2$ , and 100 mM NaCl), added to scintillation liquid (30% LSC Scintisafe Mixture), and counted in a scintillation counter (LS6500 Multipurpose Scintillation counter).

### Crystallization, data collection and structure analysis

The  $\alpha T^*(G56P)$  mutant complexed with GDP, at 10 mg/ml in 50 mM Na-cacodylate buffer (pH 6.5), was crystallized by the hanging-drop vapor-diffusion method in 1.8-2.1 M ammonium sulfate  $(\text{NH}_4)_2\text{SO}_4$ . Crystals (0.2 mm  $\times$  0.5 mm  $\times$  0.5 mm) grew in 5-7 days at  $20^\circ\text{C}$  and belonged to the space group  $P4_32_12$  ( $a=b=97.2$  Å,  $c=380.6$  Å;  $\alpha=\beta=\gamma=90^\circ$ ). For data collection at 100 K, crystals were transferred to a well solution supplemented with

2.5-3.0 M  $(\text{NH}_4)_2\text{SO}_4$  for 30-60 seconds, followed by flash freezing in a liquid nitrogen stream immediately before the data collection. Freezing the crystals by any other method or in any other cryoprotectant led to their disintegration. The data sets were collected at beam line A1 at MacCHESS, Cornell University, with an ADSC Quantum-210 CCD detector (four  $2048 \times 2048$ -pixel modules). The data sets were indexed and processed using HKL2000.<sup>37</sup> The structure was determined by molecular replacement using the coordinates from 1TAG ( $\alpha\text{T-GDP-Mg}^{2+}$ ) as a search model in Molrep from the CCP4 suite (<http://www.ccp4.ac.uk>). CNS was utilized to obtain simulated annealing-generated models for  $\alpha\text{T}^*(\text{G56P})\text{-GDP}$ . Model building was performed in Coot.<sup>38</sup> Different parts of the protein and bound nucleotide were fitted into the observed densities followed by refinement using Refmac5 in CCP4 as well as a combination of rigid-body, simulated annealing, energy minimization, and B-factor protocols in CNS.<sup>39</sup> The structural superposition was done using the program LSQMAN<sup>40</sup> for superimposing the Ca carbon backbone in Coot. The contact and other coordinate analyses were done using the CCP4 suite. All structural images were made with PyMOL (<http://www.pymol.org>). Structure factors and coordinates are deposited in the Research Collaboratory for Structural Bioinformatics (RCSB) protein database with PDB code 3V00.

## Results

### The R\*-dependent activation of $\alpha\text{T}^*(\text{G56P})$ is less sensitive to $\beta 1\gamma 1$

$\alpha\text{T}^*(\text{WT})$  is capable of only a very slow rate of spontaneous GDP-GTP exchange (Figure 1A, inverted triangles), whereas the  $\alpha\text{T}^*(\text{G56P})$  mutant exhibits a much more rapid rate of intrinsic nucleotide exchange (Figure 1B, inverted triangles), consistent with previous results from our laboratory.<sup>25</sup> As expected, the addition of catalytic amounts of R\* together with the  $\beta 1\gamma 1$  complex enabled  $\alpha\text{T}^*(\text{WT})$  to achieve high rates of GDP-GTP exchange (Figure 1A, open circles). The presence of relatively high concentrations of R\* has been shown to circumvent the requirement for  $\beta 1\gamma 1$  to increase the affinity of R\* for  $\alpha\text{T}$ .<sup>41</sup> Thus, increasing the levels of R\* from 20 nM to 200 nM, in the absence of the  $\beta 1\gamma 1$  subunit complex, caused a significant enhancement in the rate of GDP-GTP exchange on  $\alpha\text{T}^*(\text{WT})$  (compare Figures 1A and 1C, closed circles). Still, the addition of  $\beta 1\gamma 1$  to the above assay incubations stimulated even faster rates of GDP-GTP exchange (Figures 1A and 1C, open circles), consistent with the idea that the  $\beta 1\gamma 1$  complex plays a direct role in the R\*-dependent activation event.<sup>36-40</sup> The  $\alpha\text{T}^*(\text{G56P})$  subunit showed only a slight increase in the rate of GDP-GTP exchange when the concentration of R\* was increased from 20 nM to 200 nM in the absence of  $\beta 1\gamma 1$  (Figures 1B and 1D, closed circles). In the presence of catalytic amounts of R\* (20 nM), the addition of  $\beta 1\gamma 1$  to  $\alpha\text{T}^*(\text{G56P})$  triggered an increase in the rate of GDP-GTP exchange (Figure 1B, open circles). However, surprisingly, when the assay was performed in the presence of 200 nM R\*, the  $\beta 1\gamma 1$  complex conferred only a minor enhancement in the rate of nucleotide exchange on the  $\alpha\text{T}^*(\text{G56P})$  mutant (Figure 1D, open circles). These results seemed to suggest that although the  $\beta 1\gamma 1$  complex might help to enhance the binding of  $\alpha\text{T}^*(\text{G56P})$  to R\* at relatively low levels of R\*, consistent with the known role of G $\beta\gamma$  complexes in increasing the affinity of GPCRs for their cognate G $\alpha$  partners, it does not appear to significantly influence the actual GDP-GTP exchange event on  $\alpha\text{T}^*(\text{G56P})$ , unlike the case for  $\alpha\text{T}^*(\text{WT})$ . This suggested that the  $\alpha\text{T}^*(\text{G56P})$  mutant might resemble a conformation normally induced within  $\alpha\text{T}^*(\text{WT})$  by  $\beta 1\gamma 1$  during the course of R\*-stimulated GDP-GTP exchange. Therefore, we set out to determine the three-dimensional x-ray crystal structure of  $\alpha\text{T}^*(\text{G56P})$  as a means of potentially obtaining some insights into the structural changes induced by the  $\beta 1\gamma 1$  complex upon the  $\alpha\text{T}$  subunit, during the R\*-dependent activation process.

## General features of the x-ray structure of the $\alpha T^*(G56P)$ mutant

The x-ray crystal structure of the  $\alpha T^*(G56P)$  mutant was solved to a resolution of 2.9 Å. The data collection and refinement statistics are shown in Table 1. The  $\alpha T^*(G56P)$  structure exhibits the two major domains characteristic of  $G\alpha$  subunits (Figure 2A): one that is comprised of  $\alpha$ -helices, referred to as the helical domain (shown in yellow), and a second domain that exhibits an  $\alpha/\beta$  fold similar to those of GTPases belonging to the Ras superfamily, and thus referred to as the GTPase domain (shown in blue). While it has not been possible to generate suitable diffracting crystals for  $\alpha T^*(WT)$  alone (i.e. in the absence of  $\beta 1\gamma 1$ , see below), we can make comparisons between the x-ray structure for  $\alpha T^*(G56P)$  and the structure of retinal  $\alpha T$  bound to GDP (PDB ID: 1TAG), from here on referred to as  $\alpha T(WT)$ , which behaves like  $\alpha T^*(WT)$  with regard to its low intrinsic GDP-GTP exchange activity and its sensitivity to  $R^*$  and  $\beta 1\gamma 1$ .<sup>25</sup> Indeed, most of the secondary structural elements exhibited by  $\alpha T^*(G56P)$  are similar to those of  $\alpha T(WT)$ . The helical domain of  $\alpha T(WT)$  is made up of 6 helices designated  $\alpha A$  to  $\alpha F$ . In the crystal structure of  $\alpha T^*(G56P)$ , the  $\alpha B$  helix is longer by nearly one full turn at the N-terminus beginning at residue 98, instead of residue 95 in the structure of  $\alpha T(WT)$ . In addition, the amino acid residues comprising the  $\alpha B$  helix have poorly defined electron density for the side chains in the structure of  $\alpha T^*(G56P)$ , although the backbone has well-defined electron density. The GTPase domain of  $\alpha T(WT)$  is comprised of 6  $\alpha$ -helices, designated  $\alpha 1$  to  $\alpha 5$  and  $\alpha G$ , and a six-stranded  $\beta$ -sheet, with the strands designated as  $\beta 1$  to  $\beta 6$ .<sup>4,5</sup> In the x-ray structure of  $\alpha T^*(G56P)$ , the  $\alpha 2$  helix is completely disrupted, with the  $\beta 2$  strand being longer (i.e. because of residues Ile 180-Phe187) compared to that for  $\alpha T(WT)$  (residues Thr183-Phe187).

The RMSD of the Ca atoms of  $\alpha T^*(G56P)$ , when superimposed onto those from the structure of  $\alpha T(WT)$ , or  $\alpha T^*(WT)$  bound to the  $\beta 1\gamma 1$  complex, were 1.9 Å and 1.5 Å, respectively. Structural differences were observed in various regions of the  $\alpha T^*(G56P)$  mutant when compared to  $\alpha T(WT)$ . These are depicted in a plot of the RMSD of Ca atoms of  $\alpha T^*(G56P)$  when superimposed against  $\alpha T(WT)$  (Figure 2B), or  $\alpha T^*(WT)$  bound to the  $\beta 1\gamma 1$  complex (Figure 2C). Therefore, while the overall structure of  $\alpha T^*(G56P)$  is similar to that of other  $G\alpha$  subunits, there are some noteworthy differences, which as discussed below, might shed light on the nature of the conformational changes induced in the  $\alpha T(WT)$  subunit by the combined actions of  $R^*$  and the  $\beta 1\gamma 1$  subunit complex during the G protein activation event.

## Arg174 and Lys266 show weaker interactions with GDP in the $\alpha T^*(G56P)$

The x-ray structure of the  $\alpha T^*(G56P)$  mutant contains a bound GDP molecule. The fact that this mutant exhibits a significantly faster rate of spontaneous GDP-GTP exchange compared to  $\alpha T(WT)$  (or  $\alpha T^*(WT)$ ), implies that its interactions with GDP are in some way weakened, particularly given that GDP dissociation is the rate-limiting step for G protein activation. In general, the amino acid residues that interact with GDP in the x-ray structure for  $\alpha T^*(G56P)$  are similar to those responsible for binding guanine nucleotides in  $\alpha T(WT)$  (Figure 3A). However, two interactions appear to be different. One involves Arg174, which in the x-ray structure of  $\alpha T(WT)$ , is hydrogen-bonded through its side-chain guanidinium groups to the  $\alpha$ - and  $\beta$ -oxygens of the phosphate groups of GDP (Figure 3B). What is especially interesting about this difference is that a similar change was observed for the corresponding residue (Arg178) in the x-ray crystal structure of a mutant form of  $G\alpha i 1$ , in which the threonine residue at position 329 was mutated to an alanine (i.e.  $G\alpha i 1(T329A)$ ).<sup>42</sup> This  $G\alpha i 1$  mutant exhibited an ~20-fold increase in its rate of spontaneous GDP-GTP exchange compared to wild-type  $G\alpha i 1$ , similar to the increased rate of nucleotide exchange that we see with  $\alpha T^*(G56P)$ . The second interaction with GDP that appears to be altered in the x-ray structure for  $\alpha T^*(G56P)$ , compared to  $\alpha T(WT)$ , involves Lys266. In  $\alpha T(WT)$ , this



residue helps to stabilize the guanine ring of GDP via both hydrogen bonds and hydrophobic interactions, whereas in the structure for the G56P mutant, its position would suggest that it undergoes weaker interactions with GDP (Figure 3B). These differences between Arg174, Lys266, and GDP likely contribute to the ability of  $\alpha T^*(G56P)$  to undergo much more rapid GDP-GTP exchange compared to the  $\alpha T(WT)$  subunit.

### **The switch regions of GDP-bound $\alpha T^*(G56P)$ adopt conformations that are distinct from those for GDP-bound $\alpha T(WT)$**

It is well documented from structural analyses that three regions on the  $G\alpha$  subunits (designated Switch 1-3) undergo conformational changes upon the binding of GTP, when compared to their conformations in the GDP-bound state.<sup>5,6</sup> The x-ray crystal structure of the GDP-bound  $\alpha T^*(G56P)$  subunit shows that each of the three switch regions exhibit differences when compared to their conformations in the x-ray structure for GDP-bound  $\alpha T(WT)$  (Figures 2B and 2C). These differences in the switch regions do not match the changes that accompany GDP-GTP exchange and can be distinguished from the conformations of Switch 1-3 seen in the x-ray structure for GTP $\gamma$ S-bound  $\alpha T(WT)$ .<sup>5</sup> The differences in the switch domain conformations exhibited by GDP-bound  $\alpha T^*(G56P)$  (Figure 4, left panel) appear to be triggered by the loss of the hydrogen bond that is normally formed between the main-chain amide of Gly56 in  $\alpha T(WT)$  and the main-chain carbonyl of Lys50 (Figure 4, right panel). This in turn causes a change in the conformation of Linker 1 in the G56P mutant, resulting in the loss of a hydrogen bond between the main-chain amide of Tyr57 and the side-chain carboxyl oxygen of Glu167. The loss of this hydrogen bond then causes a conformational change in the adjacent Linker 2/Switch 1 region, which is transmitted to other regions of the protein. These include the following residues: amino acids 196 to 210 (Switch 2), amino acids 226 to 238 (Switch 3), amino acids 249-264, and amino acids (305-319).

The Linker 2/Switch 1 region, along with Linker 1, has been proposed to serve as a hinge around which the helical domain would need to be rotated relative to the GTPase domain, in order to achieve the accelerated release of GDP during a G protein activation event.<sup>5,25</sup> Indeed the conserved glycine residue in Linker 2/Switch 1, Gly179, shows the highest RMSD of all C $\alpha$  atoms in this region of  $\alpha T^*(G56P)$  as compared to  $\alpha T(WT)$  (Figure 2B). In addition, we have shown that the mutation of Gly179 to proline ( $\alpha T^*(G179P)$ ) results in constitutive GDP-GTP exchange, similar to the  $\alpha T^*(G56P)$  mutant.<sup>25</sup> The differences in Switch 1 exhibited by the GDP-bound  $\alpha T^*(G56P)$  mutant, as compared to GDP-bound  $\alpha T(WT)$ , appear to have an influence on Switch 2. One likely reason is due to the loss of a hydrogen-bonding interaction in the G56P mutant that normally occurs between the main-chain oxygen of Thr178 and the side-chain amino group of Lys205 in  $\alpha T(WT)$ . Several other interactions are also lost when comparing the x-ray structure of GDP-bound  $\alpha T^*(G56P)$  with that of GDP-bound  $\alpha T(WT)$  (Figure 5). These include: (1) A hydrophobic cluster that forms between Val197, Trp207 and Phe211 in  $\alpha T(WT)$  but is not evident in the  $\alpha T^*(G56P)$  structure. (2) A hydrogen bond between the main-chain carbonyl oxygen of Asp196 and the side-chain amino group of Lys206 in the structure of  $\alpha T(WT)$  that is missing in the  $\alpha T^*(G56P)$  mutant. (3) A hydrogen bond between the nitrogen atom of the indole ring of Trp207 and the main-chain carbonyl oxygen of Gly198 in  $\alpha T(WT)$  that is absent in the G56P mutant.

The loss of these interactions in the GDP-bound  $\alpha T^*(G56P)$  subunit leads to several new interactions between Switch 1 and Switch 2, as well as within the Switch 2 domain (Figure 6A). These are the following: (1) A hydrogen bond between the main-chain amide of Gly199 and the main-chain carbonyl oxygen of Thr178. (2) A hydrogen bond between the main chain amide of Ile181 and the main-chain carbonyl oxygen of Asp196. (3) A hydrogen bond between the main chain carbonyl oxygen of Ile181 and the main-chain amide nitrogen

of Asp196. (4) A hydrogen bond between the side-chain nitrogen (NH1) of Arg 201 and the side-chain oxygen (OE2) of Glu 241. Thus, the x-ray structure of the GDP-bound  $\alpha T^*(G56P)$  subunit shows the establishment of a new network of interactions between Switch 1 and Switch 2 (Figure 6A, left panel). Interestingly, Thr178 and Arg 201 from Switch 1 and Switch 2 are involved in contacting the  $G\beta$  subunit in the structure of  $\alpha T^*(WT)$  complexed with  $\beta 1\gamma 1$  (Figure 6B).<sup>11</sup> This, along with our findings that the  $\alpha T^*(G56P)$  subunit shows a reduced requirement for  $\beta 1\gamma 1$  during  $R^*$ -mediated GDP-GTP exchange, suggests that the structural differences observed in the Switch 1 and Switch 2 regions of the G56P mutant compared to  $\alpha T(WT)$  might resemble changes induced by the  $\beta 1\gamma 1$  complex in the presence of  $R^*$ . In addition, a sequence alignment of  $\alpha T$  against  $G\alpha$  subunits belonging to both the  $G_i$  family as well as other G protein families shows that all of the residues that either lose or gain interacting partners in the x-ray structure for  $\alpha T^*(G56P)$ , compared to  $\alpha T(WT)$ , are conserved. This suggests that structural changes similar to those observed in  $\alpha T^*(G56P)$  might also be occurring in other  $G\alpha$  subunits.

## Discussion

Understanding the steps that comprise the conversion of GDP-bound heterotrimeric G proteins to their GTP-bound  $G\alpha$  subunits and free  $G\beta\gamma$  complex ranks among the most fundamentally important issues in signal transduction, as these activation events are prerequisite to a host of G protein-dependent changes in second messenger levels and cellular responses. In order to develop a complete picture of how G protein activation occurs, it will be necessary to combine the information obtained from structural and biophysical analyses of GPCRs complexed to their G protein-signaling partners, with the studies of various  $G\alpha$  mutants that might mimic individual species that form along the activation reaction pathway. A major breakthrough in this regard has been provided by the x-ray crystal structure of the  $\beta$ -adrenergic receptor in complex with  $G_s$ , its cognate G protein, in its nucleotide-free state.<sup>14-16</sup> Here we describe efforts to obtain a  $G\alpha$  subunit that contains a single mutation in a linker region connecting the helical and GTPase domains, with the goal being to better understand how perturbing this linker might impact the activation event.

Our initial assumption was that by making substitutions within Linker 1 and/or Linker 2 of the  $\alpha T^*$  subunit, and in particular by changing conserved glycine residues to proline within these regions (i.e. G56P or G179P substitutions), we would alter the flexibility of the linkers that connect the GTPase and helical domains and cause a change in their relative juxtaposition. The idea being that such substitutions would help to open the “clam shell” that is formed by these two domains, and in doing so, facilitate the release of bound GDP and potentially create novel constitutively active  $G\alpha$  subunits. In fact, both the  $\alpha T^*(G56P)$  and  $\alpha T^*(G179P)$  mutants showed an enhanced ability to undergo GDP-GTP exchange in the absence of  $R^*$ , when compared to the  $\alpha T(WT)$  and  $\alpha T^*(WT)$  subunits.<sup>25</sup> However, the x-ray crystal structure that we present here for the  $\alpha T^*(G56P)$  mutant does not show a significant alteration in the relative juxtaposition of the GTPase domain relative to the helical domain, presumably because the G56P mutant has retained bound GDP which helps to maintain a “closed” conformation rather than an “open” state. This suggests that the x-ray structure for the GDP-bound form of  $\alpha T^*(G56P)$  might mimic an intermediate state along the receptor-mediated nucleotide exchange pathway which would form prior to the actual release of GDP, and therefore might offer some potentially useful insights into different aspects of the G protein activation event.

One in particular concerns the role that the  $G\beta\gamma$  complex may play in working together with an activated GPCR to help drive the activation process. There have been various suggestions that  $G\beta\gamma$  plays multiple roles in G protein activation, first by significantly enhancing the affinity of  $G\alpha$  subunits for their GPCRs, but secondly and more directly, by working

together with GPCRs to stimulate GDP-GTP exchange.<sup>30-33</sup> In one such model, the  $G\beta\gamma$  complex is proposed to function as a lever to help separate the  $\beta 3$ - $\alpha 2$  loop from Switch 1 and thereby provides an “exit route” for GDP.<sup>32</sup> A second potential mechanism for  $G\beta\gamma$  involvement, referred to as the “gear-shift” model, suggests that the amino-terminal tail of the  $G\gamma$  subunit helps to displace the helical domain from the GTPase domain and in this manner, provides an exit for GDP.<sup>33</sup> Our characterization of the  $\alpha T^*(G56P)$  mutant shows that when assaying at relatively high levels of  $R^*$ , so that the  $\alpha T^*$  subunit is no longer dependent upon the  $\beta 1\gamma 1$  complex for binding to  $R^*$ , there is little additional advantage provided by  $\beta 1\gamma 1$  in terms of stimulating GDP-GTP exchange. This is not the case when assaying  $\alpha T^*(WT)$ , as  $\beta 1\gamma 1$  provides a significant stimulation of the GDP-GTP exchange activity of  $\alpha T^*$ , even at relatively high levels of  $R^*$ . Thus, it is tempting to consider that the  $G56P$  mutant might adopt a conformation that is normally induced within  $\alpha T(WT)$  by  $\beta 1\gamma 1$  during the  $R^*$ -stimulated activation reaction. In particular, the structural differences observed in the Switch 1 and Switch 2 regions of  $\alpha T^*(G56P)$ , as compared to the switch regions of  $\alpha T(WT)$ , might reflect the types of changes mediated by  $\beta 1\gamma 1$  if it were acting as proposed in the lever model to help stimulate GDP-GTP exchange and G protein-activation. These changes in Switch 1 and Switch 2 would also be consistent with the idea that  $G\alpha$  subunits adopt a “pre-activated” conformation when bound to  $G\beta\gamma$ , presumably to help stabilize the GTP-bound state following nucleotide exchange.<sup>30</sup>

Another potentially interesting possibility that arises from an analysis of the x-ray crystal structure of the  $\alpha T^*(G56P)$  mutant concerns how the helical domains of  $G\alpha$  subunits might communicate with their carboxyl terminal regions that contain the putative contact sites for GPCRs and represent the starting point for the signal that triggers GDP release and its exchange for GTP. Specifically, it has been suggested that an activated GPCR, by contacting the  $\alpha 4/\beta 6$  loop of a  $G\alpha$  subunit, induces a rotation and translation of the  $\alpha 5$  helix and concomitant conformational changes in the  $\beta 6$  strand. These conformational changes would then be transmitted to the  $\beta 6/\alpha 5$  loop, which makes contact with the guanine ring of GDP via the conserved TCAT motif, thereby influencing the hold on GDP. However, starting with the initial descriptions of the x-ray crystal structures for  $G\alpha$  subunits, and the realization that the helical domain folds over the nucleotide bound to the GTPase domain (i.e. to form a “clam shell”), it has been assumed that the GPCR-mediated activation event would necessitate an opening of the clam shell such that GDP was free to exit from  $G\alpha$ . Indeed, a recent study using site-directed spin labeling and electron-electron resonance spectroscopy suggested that GPCR-catalyzed nucleotide exchange in G proteins requires large-scale changes in the relative orientation of the helical and GTPase domains.<sup>27</sup> Also, in the aforementioned structure of the nucleotide-free form of the  $G_s$  heterotrimer complexed to the  $\beta 2$ -adrenergic receptor, the helical domain is rotated by  $\sim 120^\circ$  relative to the Ras-like GTPase domain, compared to the x-ray crystal structure of  $\alpha s$  complexed to  $GTP\gamma S$ .<sup>14-16</sup>

The lack of the availability of an x-ray structure of  $G\alpha s$  complexed to GDP makes it difficult to map out the conformational changes that occur in the switch regions in the case of the  $\beta$ -adrenergic receptor-induced release of GDP. This also prevented a direct mapping of the conformational changes that occur in the  $\alpha T^*(G56P)$ , compared to those of  $\alpha T(WT)$ , onto the structure of the complex of the  $\beta 2$ -adrenergic receptor and the  $G_s$  heterotrimer. The x-ray structure of the  $\alpha T^*(G56P)$  mutant demonstrates how a series of conformational transitions occur in response to a single substitution within the linker region that connects the helical domain to the GTPase domain. These changes proceed through the Switch 1 and Switch 2 regions and continue through Switch 3 to residues 305-319 comprising the  $\alpha 4/\beta 6$  loop and the  $\beta 6$  strand. It is possible that the engagement of GPCRs with the carboxyl-terminal region of  $G\alpha$  subunits could initiate a similar set of changes, but in reverse order relative to what we see with the  $\alpha T^*(G56P)$  mutant, thereby providing a conformational connection between the GPCR-binding site and the helical domain on  $G\alpha$  subunits. As we



learn more about the distinct species that form along the G protein activation pathway, we can expect that the roles played by GPCRs and G $\beta\gamma$  complexes in the actual GDP-GTP exchange event, as well as the potential involvement of G $\beta\gamma$  in helping G $\alpha$  subunits assume a GTP-bound activated state, will become much better defined. The insights gained from these studies, together with future structure-function analyses of additional G $\alpha$  mutants that reflect intermediate states in the G protein activation process, should ultimately provide us with a more comprehensive picture for this critically important event in signal transduction.

## Acknowledgments

We would like to acknowledge Cindy Westmiller for her expert secretarial assistance.

This work was supported by National Institutes of Health grant R01 GM047458 and by resources provided by MacCHESS (RR001646).

## References

1. Burns ME, Arshavsky VY. Beyond counting photons: trials and trends in vertebrate visual transduction. *Neuron*. 2005; 48:387–401. [PubMed: 16269358]
2. Chen CK. The vertebrate phototransduction cascade: amplification and termination mechanisms. *Rev Physiol Biochem Pharmacol*. 2005; 154:101–121. [PubMed: 16634148]
3. He W, Cowan CW, Wensel TG. RGS9, a GTPase accelerator for phototransduction. *Neuron*. 1998; 20:95–102. [PubMed: 9459445]
4. Noel JP, Hamm HE, Sigler PB. The 2.2 Å crystal structure of transducin- $\alpha$  complexed with GTP $\gamma$ S. *Nature*. 1993; 366:654–663. [PubMed: 8259210]
5. Lambright DG, Noel JP, Hamm HE, Sigler PB. Structural determinants for activation of the  $\alpha$ -subunit of a heterotrimeric G protein. *Nature*. 1994; 369:621–628. [PubMed: 8208289]
6. Mixon MB, Lee E, Coleman DE, Berghuis AM, Gilman AG, Sprang SR. Tertiary and quaternary structural changes in G $_{i\alpha 1}$  induced by GTP hydrolysis. *Science*. 1995; 270:954–960. [PubMed: 7481799]
7. Sunahara RK, Tesmer JJ, Gilman AG, Sprang SR. Crystal structure of the adenylyl cyclase activator G $_{s\alpha}$ . *Science*. 1997; 278:1943–1947. [PubMed: 9395396]
8. Kreutz B, Yau DM, Nance MR, Tanabe S, Tesmer JJ, Kozasa T. A new approach to producing functional G $\alpha$  subunits yields the activated and deactivated structures of G $\alpha_{12/13}$  proteins. *Biochemistry*. 2006; 45:167–174. [PubMed: 16388592]
9. Slep KC, Kercher MA, Wieland T, Chen CK, Simon MI, Sigler PB. Molecular architecture of G $\alpha_o$  and the structural basis for RGS16-mediated deactivation. *Proc Natl Acad Sci USA*. 2008; 105:6243–6248. [PubMed: 18434540]
10. Wall MA, Coleman DE, Lee E, Iniguez-Lluhi JA, Posner BA, Gilman AG, Sprang SR. The structure of the G protein heterotrimer G $_{i\alpha 1}\beta_1\gamma_2$ . *Cell*. 1995; 83:1047–1058. [PubMed: 8521505]
11. Lambright DG, Sondek J, Bohm A, Skiba NP, Hamm HE, Sigler PB. The 2.0 Å crystal structure of a heterotrimeric G protein. *Nature*. 1996; 379:311–319. [PubMed: 8552184]
12. Slep KC, Kercher MA, He W, Cowan CW, Wensel TG, Sigler PB. Structural determinants for regulation of phosphodiesterase by a G protein at 2.0 Å. *Nature*. 2001; 409:1071–1077. [PubMed: 11234020]
13. Tesmer JJ, Sunahara RK, Gilman AG, Sprang SR. Crystal structure of the catalytic domains of adenylyl cyclase in a complex with G $_{s\alpha}$ .GTP $\gamma$ S. *Science*. 1997; 278:1907–1916. [PubMed: 9417641]
14. Rasmussen SG, DeVree BT, Zou Y, Kruse AC, Chung KY, Kobilka TS, Thian FS, Chae PS, Pardon E, Calinski D, Mathiesen JM, Shah ST, Lyons JA, Caffrey M, Gellman SH, Steyaert J, Skiniotis G, Weis WI, Sunahara RK, Kobilka BK. Crystal structure of the  $\beta_2$  adrenergic receptor-Gs protein complex. *Nature*. 2011; 477:549–555. [PubMed: 21772288]
15. Westfield GH, Rasmussen SG, Su M, Dutta S, DeVree BT, Chung KY, Calinski D, Velez-Ruiz G, Oleskie AN, Pardon E, Chae PS, Liu T, Li S, Woods VL Jr, Steyaert J, Kobilka BK, Sunahara RK,

- Skiniotis G. Structural flexibility of the G $\alpha$ s  $\alpha$ -helical domain in the  $\beta_2$ -adrenoceptor Gs complex. *Proc Natl Acad Sci USA*. 2011; 108:16086–16091. [PubMed: 21914848]
16. Chung KY, Rasmussen SG, Liu T, Li S, DeVree BT, Chae PS, Calinski D, Kobilka BK, Woods VL Jr, Sunahara RK. Conformational changes in the G protein Gs induced by the  $\beta_2$  adrenergic receptor. *Nature*. 2011; 477:611–615. [PubMed: 21956331]
  17. Hamm HE, Deretic D, Arendt A, Hargrave PA, Koenig B, Hofmann KP. Site of G protein binding to rhodopsin mapped with synthetic peptides from the  $\alpha$  subunit. *Science*. 1988; 241:832–835. [PubMed: 3136547]
  18. Osawa S, Weiss ER. The effect of carboxyl-terminal mutagenesis of G $\alpha$  on rhodopsin and guanine nucleotide binding. *J Biol Chem*. 1995; 270:31052–31058. [PubMed: 8537363]
  19. Sullivan KA, Miller RT, Masters SB, Beiderman B, Heideman W, Bourne HR. Identification of receptor contact site involved in receptor-G protein coupling. *Nature*. 1987; 330:758–760. [PubMed: 2827032]
  20. West RE, Moss J, Vaughan M, Liu T, Liu TY. Pertussis toxin-catalyzed ADP-ribosylation of transducin Cysteine 347 is the ADP-ribose acceptor site. *J Biol Chem*. 1985; 260:14428–14430. [PubMed: 3863818]
  21. Fotiadis D, Liang Y, Filipek S, Saperstein DA, Engel A, Palczewski K. The G protein-coupled receptor rhodopsin in the native membrane. *FEBS Lett*. 2004; 564:281–288. [PubMed: 15111110]
  22. Marin EP, Krishna AG, Sakmar TP. Rapid activation of transducin by mutations distant from the nucleotide-binding site: evidence for a mechanistic model of receptor-catalyzed nucleotide exchange by G proteins. *J Biol Chem*. 2001; 276:27400–27405. [PubMed: 11356823]
  23. Marin EP, Krishna AG, Sakmar TP. Disruption of the  $\alpha$ 5 helix of transducin impairs rhodopsin-catalyzed nucleotide exchange. *Biochemistry*. 2002; 41:6988–6994. [PubMed: 12033931]
  24. Posner BA, Mixon MB, Wall MA, Sprang SR, Gilman AG. The A326S mutant of G $\alpha_{i1}$  as an approximation of the receptor-bound state. *J Biol Chem*. 1998; 273:21752–21758. [PubMed: 9705312]
  25. Majumdar S, Ramachandran S, Cerione RA. Perturbing the linker regions of the  $\alpha$ -subunit of transducin: a new class of constitutively active GTP-binding proteins. *J Biol Chem*. 2004; 279:40137–40145. [PubMed: 15271992]
  26. Oldham WM, Van Eps N, Preininger AM, Hubbell WL, Hamm HE. Mechanism of the receptor-catalyzed activation of heterotrimeric G proteins. *Nat Struct Mol Biol*. 2006; 13:772–777. [PubMed: 16892066]
  27. Van Eps N, Preininger AM, Alexander N, Kaya AI, Meier S, Meiler J, Hamm HE, Hubbell WL. Interaction of a G protein with an activated receptor opens the interdomain interface in the  $\alpha$  subunit. *Proc Natl Acad Sci USA*. 2011; 108:9420–9424. [PubMed: 21606326]
  28. Herrmann R, Heck M, Henklein P, Hofmann KP, Ernst OP. Signal transfer from GPCRs to G proteins: role of the G $\alpha$  N-terminal region in rhodopsin-transducin coupling. *J Biol Chem*. 2006; 281:30234–30241. [PubMed: 16847064]
  29. Ceruso MA, Periolo X, Weinstein H. Molecular dynamics simulations of transducin: interdomain and front to back communication in activation and nucleotide exchange. *J Mol Biol*. 2004; 338:469–481. [PubMed: 15081806]
  30. Abdulaev NG, Ngo T, Zhang C, Dinh A, Brabazon DM, Ridge KD, Marino JP. Heterotrimeric G-protein  $\alpha$ -subunit adopts a “preactivated” conformation when associated with  $\beta\gamma$ -subunits. *J Biol Chem*. 2005; 280:38071–38080. [PubMed: 16129667]
  31. Oldham WM, Van Eps N, Preininger AM, Hubbell WL, Hamm HE. Mapping allosteric connections from the receptor to the nucleotide-binding pocket of heterotrimeric G proteins. *Proc Natl Acad Sci USA*. 2007; 104:7927–7932. [PubMed: 17463080]
  32. Iiri T, Farfel Z, Bourne HR. G-protein diseases furnish a model for the turn-on switch. *Nature*. 1998; 394:35–38. [PubMed: 9665125]
  33. Cherfils J, Chabre M. Activation of G-protein G $\alpha$  subunits by receptors through G $\alpha$ -G $\beta$  and G $\alpha$ -G $\gamma$  interactions. *Trends Biochem Sci*. 2003; 28:13–17. [PubMed: 12517447]
  34. Rondard P, Iiri T, Srinivasan S, Meng E, Fujita T, Bourne HR. Mutant G protein  $\alpha$  subunit activated by G $\beta\gamma$ : a model for receptor activation. *Proc Natl Acad Sci USA*. 2001; 98:6150–6155. [PubMed: 11344266]

35. Skiba NP, Bae H, Hamm HE. Mapping of effector binding sites of transducin  $\alpha$ -subunit using  $G_{\alpha t}/G_{\alpha i1}$  chimeras. *J Biol Chem.* 1996; 271:413–424. [PubMed: 8550597]
36. Min KC, Gravina SA, Sakmar TP. Reconstitution of the vertebrate visual cascade using recombinant heterotrimeric transducin purified from Sf9 cells. *Protein Expr Purif.* 2000; 20:514–526. [PubMed: 11087692]
37. Otwinowski, Z.; Minor, W. Processing of X-ray Diffraction Data Collected in Oscillation Mode. In: Carter, CW., Jr; Sweet, RM., editors. *Methods Enzymology.* Vol. 276: Macromolecular Crystallography, part A. Academic Press; New York: 1997. p. 307-326.
38. Emsley P, Cowtan K. Coot: model-building tools for molecular graphics. *Acta Crystallogr D Biol Crystallogr.* 2004; 60:2126–2132. [PubMed: 15572765]
39. Brunger AT, Adams PD, Clore GM, DeLano WL, Gros P, Grosse-Kunstleve RW, Jiang JS, Kuszewski J, Nilges M, Pannu NS, Read RJ, Rice LM, Simonson T, Warren GL. Crystallography & NMR system: A new software suite for macromolecular structure determination. *Acta Crystallogr D Biol Crystallogr.* 1998; 54:905–921. [PubMed: 9757107]
40. Kleywegt GJ. Use of non-crystallographic symmetry in protein structure refinement. *Acta Crystallogr D Biol Crystallogr.* 1996; 52:842–857. [PubMed: 15299650]
41. Phillips WJ, Wong SC, Cerione RA. Rhodopsin/transducin interactions. II Influence of the transducin- $\beta\gamma$  subunit complex on the coupling of the transducin- $\alpha$  subunit to rhodopsin. *J Biol Chem.* 1992; 267:17040–17046. [PubMed: 1512243]
42. Kapoor N, Menon ST, Chauhan R, Sachdev P, Sakmar TP. Structural evidence for a sequential release mechanism for activation of heterotrimeric G proteins. *J Mol Biol.* 2009; 393:882–897. [PubMed: 19703466]
43. Wallace AC, Laskowski RA, Thornton JM. LIGPLOT: a program to generate schematic diagrams of protein-ligand interactions. *Protein Eng.* 1996; 8:127–134. [PubMed: 7630882]

## Abbreviations

|                                  |   |
|----------------------------------|---|
| <b>G<math>\alpha</math></b>      | G protein alpha subunit   |
| <b><math>\alpha</math>T</b>      | G protein alpha subunit of the vertebrate vision system (transducin)                      |
| <b>GDP</b>                       | Guanosine diphosphate   |
| <b>GTP</b>                       | Guanosine triphosphate  |
| <b>G<math>\beta\gamma</math></b> | G protein beta gamma subunit complex  |
| <b>GPCRs</b>                     | G protein-coupled receptors   |
| <b>G protein</b>                 | Guanine nucleotide binding protein  |
| <b>PDE</b>                       | cyclic-GMP phosphodiesterase  |
| <b>EPR</b>                       | Electron paramagnetic resonance   |
| <b>HEPES</b>                     | 4-(2-hydroxyethyl)-6-sulfonic acid  |
| <b>MacCHESS</b>                  | Macromolecular Crystallography Facility at CHESS (Cornell High Energy Synchrotron Source) |
| <b>CCP4</b>                      | Comprehensive computing suite for protein crystallography                                 |
| <b>CNS</b>                       | Crystallography and NMR (Nuclear Magnetic Resonance) system                               |
| <b>RMSD</b>                      | Root mean square deviation  |
| <b>PDB</b>                       | Protein Data Bank   |

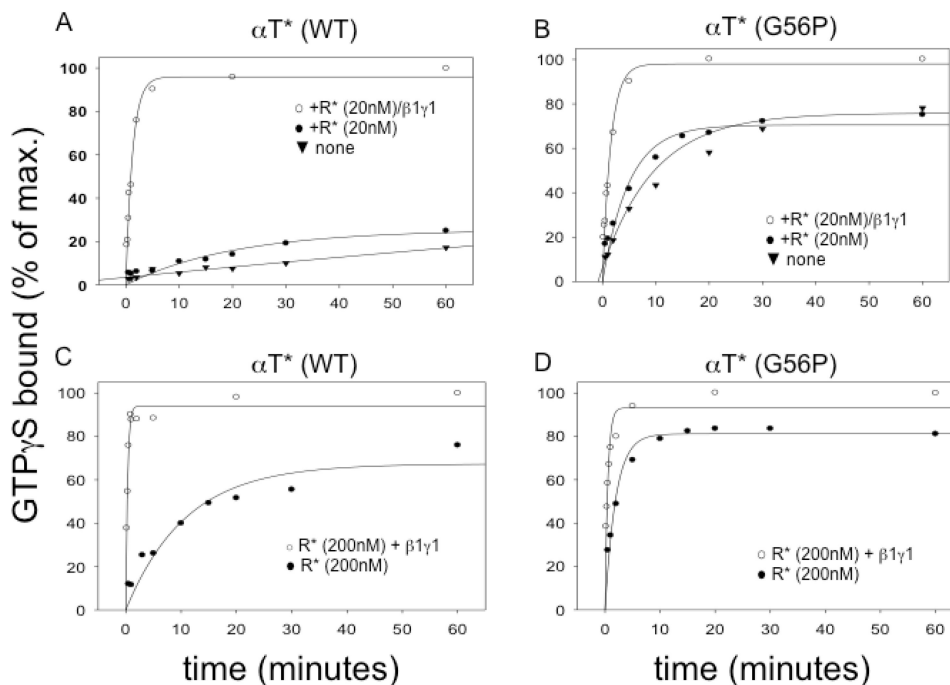


**Figure 1.**

Comparison of the rhodopsin-dependence of nucleotide exchange on  $\alpha$ T\* and  $\alpha$ T\*(G56P). 5  $\mu$ M [ $^{35}$ S] GTP $\gamma$ S (specific activity, 1 Ci/mmol) was added to 700 nM  $\alpha$ \*T (G56P) or wild-type  $\alpha$ T\*(WT), preincubated with G $\beta$  $\gamma$  (350 nM) and different concentrations of R\* (20 nM; A, B), (200 nM; C, D) in 200  $\mu$ l HMDM buffer. R\* (solubilized in 0.01% dodecyl maltoside) was activated in ambient light on ice for 5 min. Aliquots (20  $\mu$ l) of reaction mixture were removed at the indicated times and added directly to pre-wetted nitrocellulose filters on a suction manifold to quench the reaction. The filters were subsequently washed twice with HM buffer and added to 3 ml of scintillation fluid and counted on a scintillation counter. The extent of binding is plotted as percentage of maximal binding for each of the  $\alpha$ T\* subunits.

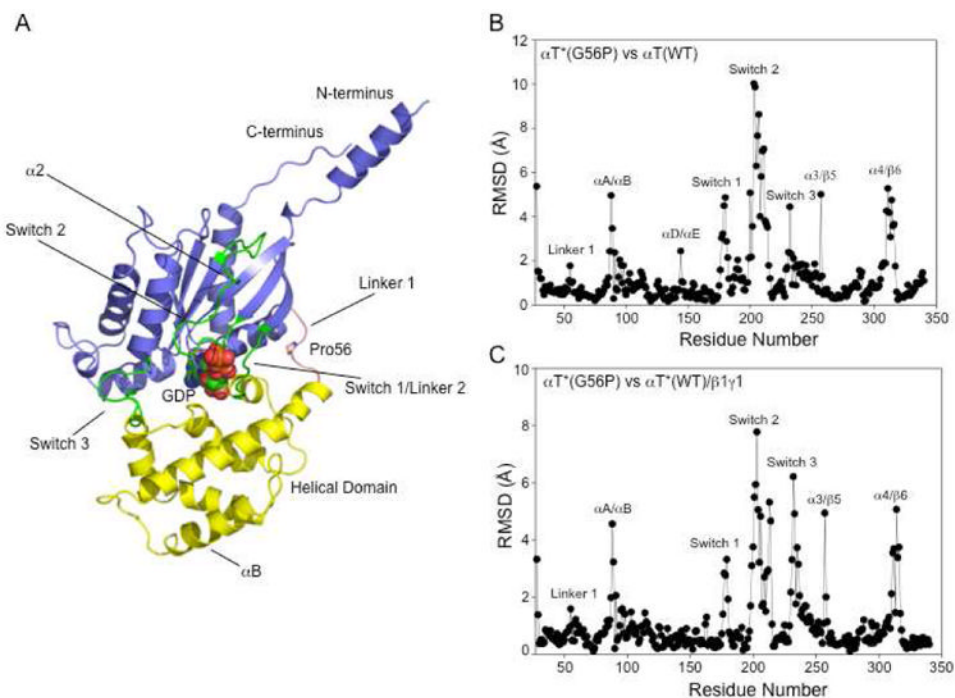


**Figure 2.** Structural changes in  $\alpha T^*(G56P)$ . (A) The overall structure of  $\alpha T^*(G56P)$  showing the GTPase (colored purple), helical domains (colored yellow), and GDP (shown as spheres). The switch regions are colored green and the Linker 1 is colored pink. (B) Plot of the root mean square difference (RMSD) between the superimposed C $\alpha$  atoms of  $\alpha T^*(G56P)$  and that of the corresponding C $\alpha$  atoms of  $\alpha T(WT)$  (PDB entry 1TAG). (C) Plot of the RMSD between the superimposed C $\alpha$  atoms of  $\alpha T^*(G56P)$  and that of the corresponding C $\alpha$  atoms of  $\alpha T(WT)$  in complex with  $\beta 1\gamma 1$  (PDB entry 1GOT).



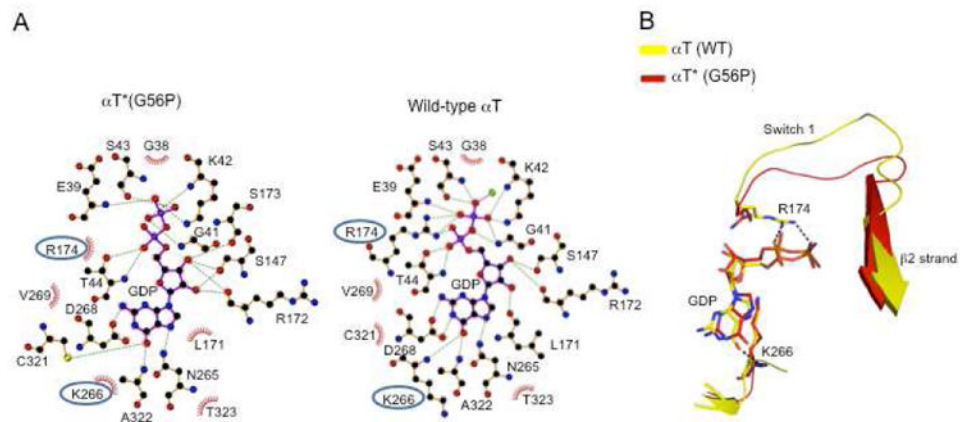


**Figure 3.**

GDP-interacting residues within  $\alpha T^*(G56P)$ . (A) Schematic view of the amino acid residues that interact with GDP in  $\alpha T^*(G56P)$  (left panel) and  $\alpha T$ (WT) (right panel) was made using the program ligplot.<sup>43</sup> Hydrogen bonded interactions are shown as dotted lines and hydrophobic interactions are shown using spoked arcs. Residues whose interactions are different between  $\alpha T$ (WT) and  $\alpha T^*(G56P)$  are circled. (B) The  $\text{Ca}$  atoms of  $\alpha T^*(G56P)$  were superimposed on  $\alpha T$ (WT). The changes in the interactions involving Arg174 and Lys266 in GDP-bound  $\alpha T$ (WT) (colored yellow) and  $\alpha T^*(G56P)$  (colored red), with the bound GDP (shown as sticks), are presented.

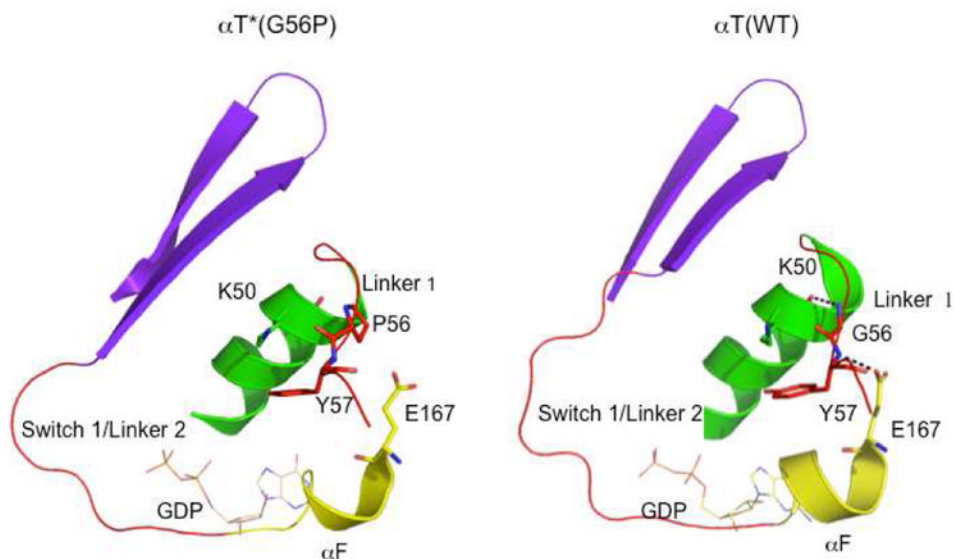


**Figure 4.** Transmission of conformational changes from Linker 1 in  $\alpha T^*(G56P)$ . The  $C\alpha$  atoms of  $\alpha T^*(G56P)$  were superimposed on the corresponding  $C\alpha$  atoms of  $\alpha T(WT)$  using the LSQMAN program. The G56P mutation results in the loss of a hydrogen-bond between the main-chain amide of Gly56 in Linker 1 and the main-chain carbonyl of Lys50 in the N-terminal helix (colored green). This in turn results in the loss of a hydrogen-bond between the main-chain amide of Tyr57 in Linker 1 and the side-chain carbonyl oxygen of Glu167 in the  $\alpha F$  helix. These interactions are shown in the  $\alpha T^*(G56P)$  structure in the left panel and in the  $\alpha T(WT)$  structure in the right panel. The hydrogen-bonding interactions are shown by dashed lines. Also, shown is the Switch 1 region as well as the  $\beta 2$  and  $\beta 3$  strands.

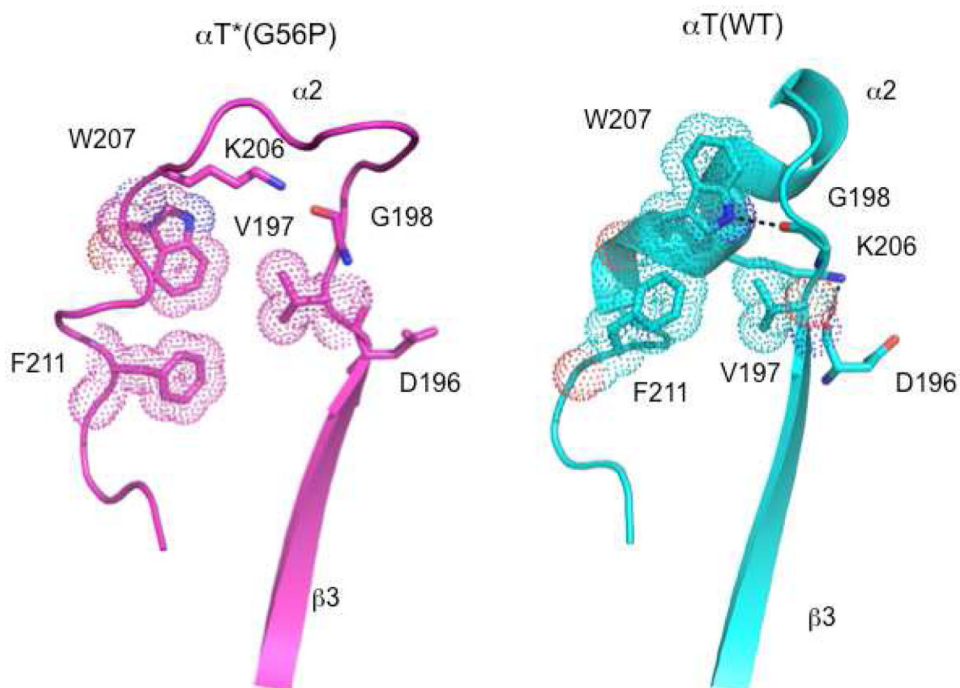


**Figure 5.** Interactions that are lost in  $\alpha T^*(G56P)$  compared to  $\alpha T(WT)$ . The  $C\alpha$  atoms of  $\alpha T^*(G56P)$  were superimposed on the corresponding  $C\alpha$  atoms of  $\alpha T(WT)$  using the LSQMAN program. A hydrophobic cluster (shown as dots) that forms between Trp207, Val197 and F211 in  $\alpha T(WT)$  (right panel) is weakened in  $\alpha T^*(G56P)$  (left panel). Also, shown is the hydrogen bond (dashed lines) between the nitrogen atom of the indole ring of Trp207 and the main-chain carbonyl oxygen of Gly198 in  $\alpha T(WT)$  (right panel), that is absent in  $\alpha T^*(G56P)$  (left panel).

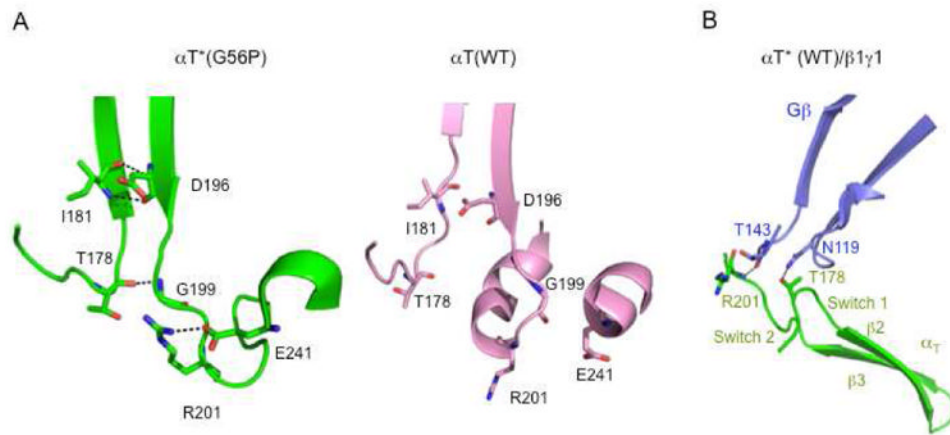


**Figure 6.**

Interactions that are gained in  $\alpha T^*(G56P)$  compared to  $\alpha T(WT)$ . The  $C\alpha$  atoms of  $\alpha T^*(G56P)$  were superimposed on to  $\alpha T(WT)$ , or  $\alpha T(WT)$  complexed to  $\beta 1\gamma 1$  using the LSQMAN program. (A) Hydrogen bonds are present between the following pairs of residues in  $\alpha T^*(G56P)$  (left panel, dashed lines): Gly199/Thr178, Ile181/Asp196 and Arg201/Glu241. The same region in  $\alpha T(WT)$  (right panel) shows the absence of these hydrogen bonds. (B) Hydrogen bonding between Arg201 and Thr178 in  $\alpha T(WT)$  (colored green) to residues in the  $\beta 1$  subunit (colored purple) of the  $\beta 1\gamma 1$  complex.

**Table 1**  
**Data Collection and Refinement Statistics**

|   |                          |
|---|--------------------------|
| space group                               | <i>P4<sub>3</sub>212</i> |
| unit cell <i>a, b, c</i> (Å)              | 93.2, 93.2, 380.6        |
| Unit cell <i>α, β, γ</i> (deg)            | 90.0, 90.0, 90.0         |
| resolution range (Å)                      | 50.0-2.9 <sup>a</sup>    |
| redundancy                                | 8.6                      |
| completeness (%)                          | 97.4                     |
| no. of unique reflections                 | 37430                    |
| <i>R</i> <sub>merge</sub> (%)             | 8.0                      |
| average <i>I</i> / <i>σ</i>               | 22.0                     |
| <i>R</i> <sub>cryst</sub>                 | 0.22                     |
| <i>R</i> <sub>free</sub>                  | 0.27                     |
| no. of protein atoms                      | 8381                     |
| no. of water molecules                    | 296                      |
| Wilson <i>B</i> value (Å <sup>2</sup> )   | 89.2                     |
| average <i>B</i> factor (Å <sup>2</sup> ) | 94.3                     |
| Ramachandran Plot                         |                          |
| most favored regions (%)                  | 86.7                     |
| additionally allowed (%)                  | 13.3                     |
| RMSD bond lengths (Å)                     | 0.007                    |
| RMSD bond angles (deg)                    | 1.2                      |